Developmental and Comparative Immunology 96 (2019) 27–36

Contents lists available at ScienceDirect

Developmental and Comparative Immunology

journal homepage: www.elsevier.com/locate/devcompimm

Molecular identification and antiviral function of the guanylate-binding protein (GBP) genes in the Chinese tree shrew (*Tupaia belangeri chinesis*)

Tianle Gu[a,b], Dandan Yu[a,c,d], Yu Fan[a,c,d], Yong Wu[a,b], Yu-Lin Yao[a,b], Ling Xu[a,c,d,**], Yong-Gang Yao[a,b,c,d,*]

[a] Key Laboratory of Animal Models and Human Disease Mechanisms of the Chinese Academy of Sciences & Yunnan Province, Kunming Institute of Zoology, Kunming, Yunnan, 650223, China
[b] Kunming College of Life Science, University of Chinese Academy of Sciences, Kunming, Yunnan, 650204, China
[c] Center for Excellence in Animal Evolution and Genetics, Chinese Academy of Sciences, Kunming, 650223, China
[d] Kunming Primate Research Center of the Chinese Academy of Sciences, Kunming Institute of Zoology, Chinese Academy of Sciences, Kunming, 650223, China

ARTICLE INFO

Keywords:
Tree shrew
Guanylate-binding protein
Innate immunity
Viral infection

ABSTRACT

Following viral detection and interferons (IFNs) production, several hundreds of IFN-stimulated genes (ISGs) are subsequently induced to act as direct antiviral effectors or regulators of the IFN signaling. The guanylate-binding protein (GBP) family belongs to IFN-inducible GTPases defending the host against a diverse group of invading pathogens such as parasites, bacteria and viruses. The Chinese tree shrew (*Tupaia belangeri chinese*) has been increasingly used as an alternative experimental animal to primates in studying viral infectious diseases. Hitherto, the tree shrew GBP family has not been characterized. In this study, we identified five tree shrew *GBP* genes (*tGBP1*, *tGBP2*, *tGBP4*, *tGBP5* and *tGBP7*) and characterized their antiviral activities. All these *tGBPs* were ubiquitously expressed in heart, spleen, intestines, kidney, liver, lung and brain tissues of the tree shrew. IFN-γ treatment of tree shrew primary renal cells (TSPRCs) significantly induced the mRNA expression of *tGBPs*. Infections with Newcastle disease virus (NDV), encephalomyocarditis virus (EMCV) and type 1 herpes simplex virus (HSV-1) enhanced *tGBPs* mRNA expression in TSPRCs, but had no effect on the localization of tGBP proteins in the cytoplasm. tGBP1, but not the other four tGBPs, showed antiviral activity against vesicular stomatitis virus (VSV) and HSV-1 infections. Taken together, this study provided the first-hand information of the GBP family members in the Chinese tree shrew, which might assist the development of tree shrew animal model for infectious diseases.

1. Introduction

The interferon (IFN)-mediated innate immune response provides a robust first line of defense against invading pathogens (McNab et al., 2015). After the production of IFN that was induced by the pathogen detection via pattern recognition receptors (PRRs), it induces expression of hundreds of IFN-stimulated genes (ISGs), leading to a remarkable antiviral state, effectively against positive-, negative-, and double-stranded RNA viruses, DNA viruses, and intracellular bacteria and parasites (Akira et al., 2006; Goubau et al., 2013; Schneider et al., 2014). The guanylate-binding protein family (GBP) belongs to a superfamily of the IFN-induced GTPases that includes the immunity-related GTPases (IRGs), the Myxoma proteins (Mx) and the very large inducible GTPases (VLIGs or GVINs) (Kim et al., 2012; MacMicking, 2004). The human *GBP* (*hGBP*) genes are located within one gene cluster on chromosome 1, whereas the mouse *Gbp* (*mGbp*) genes are located in two clusters on chromosomes 3 and 5 (Kim et al., 2011; Olszewski et al., 2006). GBPs have been shown to be important mediators of host defense *in vivo* against bacterial pathogens and parasites (Meunier and Broz, 2016; Pilla-Moffett et al., 2016). There is evidence that GBPs are also involved in the host innate immunity to viral infections (Pilla-Moffett et al., 2016). Overexpression of hGBP1 could control vesicular stomatitis virus (VSV), encephalomyocarditis virus (EMCV), hepatitis C virus (HCV) and Kaposi's sarcoma-associated herpesvirus (KSHV) replications in cell lines (Carter et al., 2005; Itsui et al., 2009; Li et al., 2016c; Lu et al., 2008; Zou et al., 2017). A splice variant of hGBP3 mediated anti-influenza activity through repression of the viral polymerase complex (Nordmann et al., 2012). mGbp4 could

* Corresponding author. Kunming Institute of Zoology, Chinese Academy of Sciences, 32 Jiao chang Donglu, Kunming, 650223, China.
** Corresponding author. Key Laboratory of Animal Models and Human Disease Mechanisms of the Chinese Academy of Sciences & Yunnan Province, Kunming Institute of Zoology, Kunming, Yunnan, 650223, China.
E-mail addresses: lingxu0502@yahoo.com (L. Xu), yaoyg@mail.kiz.ac.cn (Y.-G. Yao).

https://doi.org/10.1016/j.dci.2019.02.014
Received 27 December 2018; Received in revised form 19 February 2019; Accepted 19 February 2019
Available online 25 February 2019
0145-305X/

negatively regulate Sendai virus (SeV)-triggered IFN-I production by directly targeting IRF7 and inhibiting its function (Hu et al., 2011). hGBP5 had an antiviral activity to human immunodeficiency virus type 1 and influenza virus infections (Feng et al., 2017; Hotter et al., 2017; Krapp et al., 2016). Recently, Biering et al. (2017) discovered that the replication complexes of positive-sense RNA viruses were marked by the LC3 conjugation system of autophagy and targeted by GBPs to inhibit viral replication. All these lines of evidence suggested that GBPs played active roles in antiviral function.

The Chinese tree shrew is a squirrel-like animal inhabiting in the tropical shrubs or forests of South and Southeast Asia (Fan et al., 2013; Xu et al., 2013b; Yao, 2017; Zheng et al., 2014). This animal has a small body size, a low-cost of maintenance, a short reproductive cycle, and a close affinity with primates (Fan et al., 2013; Xu et al., 2013a; Yao, 2017). It has a susceptibility to a wide range of human pathogens, making it as a promising and viable experimental animal for human diseases, including metabolic diseases, brain aging, neurological and psychiatric diseases, and cancer (Fan et al., 2018; Li et al., 2018; Wei et al., 2017; Xiao et al., 2017; Yao, 2017). In the past decades, great efforts have been made to establish infectious disease animal models using the Chinese tree shrew (Tsukiyama-Kohara and Kohara, 2014; Xiao et al., 2017; Yao, 2017). For example, many reports have suggested that tree shrew is susceptible to hepatitis B virus (HBV) and HCV (Guo et al., 2018; Walter et al., 1996; Wang et al., 2012; Xie et al., 1998; Yan et al., 1996). Besides, it has been shown that tree shrew is readily infected by many other viruses, such as HSV-1 (Li et al., 2016a, 2016b), Coxsackie virus A16 (Li et al., 2014) and influenza H1N1 virus (Yang et al., 2013). However, lack of basic knowledge regarding the immune system genes of tree shrew has disabled our efforts to create a stable and successful animal model for infectious disease using this species (Yao, 2017).

In this study, we identified and characterized five *tGBP* genes and examined their tissue expression pattern in adult Chinese tree shrew. We also investigated *tGBP* expression pattern in tree shrew primary renal cells (TSPRCs) in response to different virus infections and tree shrew interferon-γ (tIFNγ) treatment. The cellular localization and antiviral activity of these tGBPs were also examined. Our results indicated that *tGBPs* have a closer relationship to *hGBPs* than to *mGbps*, and tGBP1 has a potent antiviral activity to VSV infection.

2. Materials and methods

2.1. Experimental animals and cell culture

The Chinese tree shrews (n = 5) were purchased from the experimental animal core facility of Kunming Institute of Zoology (KIZ), Chinese Academy of Sciences (CAS). After lethally anesthetized by pentobarbital, seven different tissues including heart, liver, spleen, lung, kidney, small intestine and brain of each tree shrew were collected. This study was approved by the Institutional Animal Care and Use Committee of KIZ, CAS.

The preparation and culture of TSPRCs was described in our previous studies (Xu et al., 2016; Yu et al., 2014). In brief, the kidney tissues were cut into small pieces and digested in a volume of 25 mL solution containing 1 mg/mL DNase (Sigma, AMPD1-1 KT) and 5 mg/mL collagenase type IV (Invitrogen, 17104019) for 45 min at 37 °C. After three washes with cold phosphate-buffered saline (PBS; biological industries, 0021517), the TSPRCs were resuspended and cultured at a density of 2×10^5 cells/mL in high-glucose Dulbecco's modified eagle medium (DMEM; Gibco-BRL, 11965-092) supplemented with 10% fetal bovine serum (FBS; Gibco-BRL, 10099-141) and 1 × penicillin/streptomycin (Gibco-BRL, 10378016) at 37 °C in 5% CO_2 until confluent. The TSR6 (tree shrew renal cell #6) cell line was established in our study (Gu et al., 2019), which was immortalized from TSPRCs. The HEK293 cells were introduced from Kunming Cell Bank, KIZ, CAS. The TSR6 and HEK293 cells were cultured using the same condition as for the TSPRCs.

2.2. RNA isolation and quantitative real-time PCR (RT-qPCR)

Total RNA was extracted using RNAsimple Total RNA Kit (TIANGEN, DP419) according to the manufacturer's instruction. Complementary DNA (cDNA) was synthesized by using random primer and M-MLV reverse transcriptase (Promega, M1701). RT-qPCR was performed using iTaq Universal SYBR Green Supermix (Bio-Rad, 1725124) supplemented with gene-specific primers (Table S1) on a CFX Connect Real-Time System (Bio-Rad, USA), as had been described in our previous studies (Xu et al., 2015, 2016; Yao et al., 2019; Yu et al., 2014).

We serially diluted the PCR product of the respective amplicon and used the 10^{-3} - 10^{-10} dilutions to generate the standard curve for the primer pair to quantify the target gene. The Ct values were measured relative to the corresponding standard curve. The tree shrew housekeeping gene *β-actin* was used as the reference gene for normalization.

2.3. Molecular clone and construction of overexpression vector

We designed the primers for cloning and amplification of *tGBPs* based on the predicted *tGBP* sequences of the Chinese tree shrew genome (http://www.treeshrewdb.org/) (Fan et al., 2014). In order to get a relatively intact mRNA sequence, rapid amplification of cDNA ends (RACE) was used to amplify the 5′-UTR and 3′-UTR using the SMARTer RACE cDNA Amplification Kit (Clontech, 634923) in accordance with the manufacture's instruction. The full-length mRNA of tGBPs were amplified using the cDNAs prepared from total RNA of TSPRCs that treated with tIFNγ for 8 h. Purified PCR products were cloned into the pMD 19-T simple vector (TaKaRa, 3271). We sequenced five positive clones to get the consensus sequence for each insert.

We constructed overexpression vectors for each tGBP and tIFNγ using the gene-specific primer pairs (Table S1). The PCR product was purified with the TIANquick Midi Purification Kit (TIANGEN, DP204) and was cloned into Flag-tagged pCMV-3Tag-8 plasmid. All the constructs were confirmed by sequencing. Overexpression vectors for tMAVS (Flag-tagged tMVAS) and tMITA (MYC-tagged tMITA) had been described in our previous studies (Xu et al., 2015, 2016) and were used as a positive control in this study.

2.4. Phylogenetic analysis

The protein sequences of human GBPs and mouse GBPs were retrieved from the GenBank (https://www.ncbi.nlm.nih.gov/): hGBP1 (NP_002044.2), hGBP2 (NP_004111.2), hGBP3 (AAI40838.1), hGBP4 (NP_443173.2), hGBP5 (NP_443174.1), hGBP6 (AAI31714.1), hGBP7 (NP_997281.2), mGbp1 (NP_034389.2), mGbp2 (AAD39746.1), mGbp3 (AAH19195.1), mGbp4 (NP_032646.2), mGbp5a (AAN52282.1), mGbp5b (AAA37668.1), mGbp6 (XP_011247688.1), mGbp7 (NP_663520.2), mGbp8 (NP_083785.3), mGbp9 (NP_766365.1), mGbp10 (NP_001034735.2), mGbp11 (NP_001034736.3). The protein sequences were aligned by using Muscle 3.8 (Edgar, 2004). The unrooted neighbor-joining (NJ) tree were constructed by MEGA6.0 (Tamura et al., 2013) with the Poisson model. A total of 1000 bootstrap replications were performed to determine the confidence of tree branch positions.

2.5. Western blot and immunofluorescence assay

Transfection was performed using X-tremeGENE HP (Roche, 06366546001) following the manufacture's instruction. Cells were harvested and lysed on ice in RIPA lysis buffer (Beyotime, P0013), followed by centrifugation at 12,000 g at 4 °C for 10 min to remove cell debris. The BCA protein assay kit (Beyotime, P0012) was used to determine the protein concentration. A total of 20 μg protein for each

sample was separated by a 12% (vol/vol) SDS-polyacrylamide gel and electrophoretically transferred onto a polyvinylidene difluoride membrane (Bio-Rad, L1620177). Membranes were blocked with 5% (wt/vol) bovine serum albumin (BSA) in Tris-buffered saline (TBS) supplemented with 0.1% Tween-20 (TBST) (Cell Signaling Technology, #9997) at room temperature for 2 h, then probed with antibodies against Flag (EnoGene, E12-001-1) to detect the Flag-tagged proteins, and against β-actin (EnoGene, E12-041-1) to detect endogenous β-actin overnight at 4 °C, respectively. After three washes with TBST, the membranes were incubated for 1 h with anti-mouse secondary antibody (1:10000, KPL, USA) at room temperature. The epitope was visualized by using an ECL western blot detection kit (Millipore, WBKLS0500).

For immunofluorescence assay, cells seeded in chamber slides (Thermo, 154526) were washed three times with PBS and were fixed by 4% paraformaldehyde. The fixed cells were permeated with 0.2% Triton X-100 for 15 min. After three washes (each 5 min) with PBS, cells were incubated with the primary antibody against Flag to detect the Flag-tagged proteins overnight at 4 °C. After another round of three washes with PBS, cells were incubated with the fluorescence labeled anti-mouse secondary antibody (Invitrogen, A-21207) for 1 h. Nuclei were stained by DAPI (Roche, 10236276001). Intact cells were imaged by using an Olympus FluoView™ 1000 confocal microscope (Olympus).

2.6. Virus infections

The vesicular stomatitis virus (tagged by GFP; VSV-GFP), type 1 herpes simplex virus (HSV-1), Newcastle disease virus (NDV) and Encephalomyocarditis virus (EMCV) had been described in our previous study (Xu et al., 2016). Briefly, the VSV-GFP was obtained from Xinwen Chen, Wuhan Institute of Virology, Wuhan, China, the HSV-1 was introduced from Jumin Zhou's laboratory at KIZ, the NDV was obtained from the China Institute of Veterinary Drug Control, Beijing, and the EMCV (Zhang et al., 2007) was a kind gift from Hanchun Yang, China Agricultural University, Beijing. For viral infections, cells were seeded in 24-well plates (5×10^4 cells/well) or in the chamber slides (2×10^4 cells/well), and were washed three times with PBS. Cells were then incubated with NDV at a multiplicity of infection of 1 (MOI = 1), HSV-1 (MOI = 1), VSV-GFP (MOI = 0.01) or EMCV (MOI = 1), respectively, for 1 h in DMEM without FBS, and were rinsed and cultured in fresh growth medium containing 1% FBS until harvest. We quantified the copy number of HSV-1 DNA in culture supernatant using RT-qPCR following the previously described approach (Zhang et al., 2014). The replication of VSV within the cells was quantified by using flow cytometry (Xu et al., 2016).

2.7. IFNγ (tIFN-γ) treatment

The HEK293 cells were seeded in 6-well plates (1×10^5 cells/well) and were transfected with pCMV-3tag-8 (empty vector) and pCMV-tIFNγ-3tag-8 using X-tremeGENE HP (Roche, 06366546001) following the manufacture's instruction. After 6 h of transfection, cells were washed three times with PBS, and switched to growth medium for 48 h. The culture supernatants containing tIFN-γ were collected and filtrated with 0.45 μm filter for use.

For tIFN-γ stimulation assay, the TSPRCs were seeded in 24-well plates (5×10^4 cells/well with 500 μL growth medium) for growth for 12 h, then the culture supernatant containing tIFN-γ was added to growth medium (100 μL/well). The TSPRCs were harvested at the indicated times post tIFN-γ treatment.

2.8. Knockout of tGBP1

We used the CRISPR-Cas9 system to knock out the *tGBP1* gene in TSR6 cells (Ma et al., 2018; Ran et al., 2013). The sgRNAs (tGBP1-sgRNA-F 5′ CACCGATGTTCAGAGCGTCCTGAT 3’/tGBP1-sgRNA-R 5′ AAACATCAGGACGCTCTGAACATC 3’) targeting the coding region of the *tGBP1* gene were designed by the CRISPR Design Tool (http://bioinfogp.cnb.csic.es/tools/breakingcas/index.php) (Oliveros et al., 2016). The sgRNA pair was annealed and cloned into the pX330-T7 vector (a kind gift from Dr. Ping Zheng, KIZ) expressing mCherry. The TSR6 cells were transfected with the pX330-T7 vector carrying the sgRNAs. Transfected cells expressing mCherry were sorted by flow cytometry and cultured for 48 h. Single cells were manually picked with a mouth pipette for expansion for around three weeks.

The AxyPrep Multisource Genomic DNA Miniprep Kit (Axygen, 26817KC1) was used to extract genomic DNA of the single TSR6 cells with potential knockout of *tGBP1*. The gene region spanning the sgRNA targeting sites was amplified by using primer pair (tGBP1-sgF 5′ CTC TGATAACACGTCCATG 3’/tGBP1-sgR 5′ ACTGTTCATTCCCACCTC 3’). The PCR products were sequenced using the primer tGBP1-sgF and analyzed by the DNASTAR Lasergene 7.1 (DNAS Inc., Madison, WI, USA) to screen for mutation(s). We were able to pick up a cell clone with a frameshift mutation (c.74_75insA) to disrupt the translation of tGBP1 protein. We used the human GBP1 monoclonal antibody (SANTA CRUZ, sc-53857) to probe the tGBP1, but this antibody was unfortunately not workable in our assay.

2.9. Statistical analysis

Statistical analysis was determined by using the unpaired Student's *t*-test with Prism software (GraphPad). Significant values were indicated as *, $p < 0.05$ and **, $p < 0.01$. Values were presented as mean ± standard error of mean (SEM).

3. Results

3.1. Identification of five GBP genes in the Chinese tree shrew

There were 7 members (*hGBP1* - *hGBP7*) and 11 members (*mGbp1* - *mGbp11*) of *GBPs* in human and mouse, respectively (Olszewski et al., 2006). Based on the genome sequence of the Chinese tree shrew and the tree shrew database (http://www.treeshrewdb.org) (Fan et al., 2013, 2014), we were able to identify five *GBPs* (*tGBP1*, *tGBP2*, *tGBP4*, *tGBP5*, *tGBP7*; the naming of each *tGBP* was based on the clustering pattern of tGBPs with hGBPs and mGBPs in the phylogenetic tree and their chromosomal localization) in tree shrew (Table S2). The coding region of *tGBPs* ranged from 1733 bp to 1884 bp, and the predicted proteins had a molecular weight ranged from 67 kD to 72 kD (Table S2). In the unrooted NJ tree, tGBPs had a closer relationship to hGBPs than to mGbps (Fig. 1A). All five *tGBPs* were mapped to one gene cluster on one chromosome based on the updated assembly genome of the Chinese tree shrew (authors’ unpublished data), which resembled the human GBPs cluster (Fig. 1B).

There were conserved motifs in the N-terminal of tGBPs, including the GxxxxGK(S/T), DxxG and TLRD/TVRD motifs that belong to the GTPases domain. The C-terminal of tGBPs had a relatively low sequence identity among different members, whereas the N-terminal of different tGBPs seemed to be more conserved. Only tGBP1, tGBP2 and tGBP5 contained a CaaX motif (Fig. 2), which was said to be responsible for its isoprenylation (Degrandi et al., 2007; Olszewski et al., 2006).

3.2. Tissue expression of tGBP mRNAs

The mRNA expression levels of *tGBPs* were analyzed in seven tissues from healthy adult tree shrews. *tGBPs* mRNA were ubiquitously detected in all examined tissues at a very low level according to the RT-qPCR. However, we could not obtain full-length *tGBP* mRNA sequences using these cDNAs as the template for PCR, suggesting that the full-length *tGBP* mRNAs were expressed at extremely low level. There was a seemingly tissue-specific pattern for the mRNA levels of *tGBPs* in healthy animals. In particular, *tGBP1* had a relatively higher mRNA level in lung compared to other tissues (Fig. 3A). *tGBP2* exhibited a

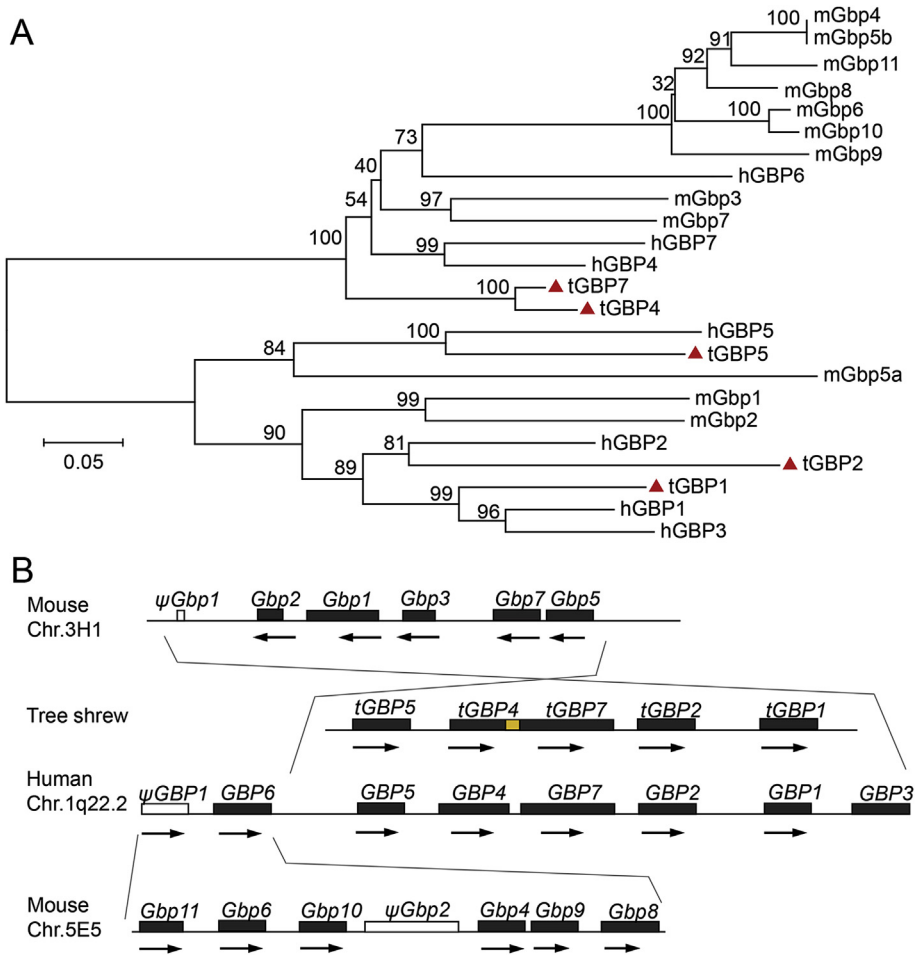

Fig. 1. Phylogenetic tree and chromosomal clustering of *hGBPs*, *mGbps* and *tGBPs*. (A) Phylogenetic tree of the GBP protein sequences of human (h), mouse (m) and the Chinese tree shrew (t). The unrooted tree was constructed using the neighbor-joining (NJ) method, with 1000 bootstrap replications. The bootstrap values for respective nodes were shown on the branches. The branch length, as measured by the scale bar, was based on the evolutionary distances used to infer the clustering pattern. The evolutionary distances were computed using the Poisson correction method. Red triangle indicated tGBPs. (B) Chromosomal clustering of hGBPs, mGbps and tGBPs. Arrows indicate the directions of transcription. Black block, individual gene. White block, pseudogene. Yellow block, exon shared by *tGBP4* and *tGBP7*. Gray lines indicated regions of synteny between human chromosome 1 and murine chromosomes 3 and 5. (For interpretation of the references to colour in this figure legend, the reader is referred to the Web version of this article.)

higher mRNA level in heart and spleen tissues compared to other tissues (Fig. 3B). *tGBP4* was highly expressed in heart, spleen, liver and lung tissues (Fig. 3C). *tGBP5* had a higher mRNA level in spleen tissues relative the other tissues (Fig. 3D), whereas *tGBP7* was highly expressed in heart and lung tissues (Fig. 3E). The different tissue expression pattern of *tGBPs* might be relevant to the specific roles of tGBPs in the immune system and further studies should be performed to characterize the underpinnings of the unique expression pattern.

3.3. Upregulation of tGBPs in TSPRCs by tree shrew IFN-γ (tIFN-γ)

The *GBP* genes belong to the dynamin-like GTPases superfamily and are prominently induced by IFN-γ in human and mouse (Meunier and Broz, 2016; Pilla-Moffett et al., 2016). We investigated whether the *tGBPs* could be induced by tIFN-γ. As the IFNs exerted their function in an autocrine or paracrine manner (Borden et al., 2007), we overexpressed the tIFN-γ in HEK293T cells and collected the culture supernatant to treat TSPRCs. tIFN-γ treatment significantly upregulated the mRNA expression levels of *tGBPs* as early as at 4 h. Notably, the most predominantly induced *tGBP5* was upregulated by nearly 70 folds at 24 h after tIFN-γ treatment compared to untreated cells (Fig. 4). These results showed that the IFN-γ inducible property of *GBPs* was conserved in tree shrew and was similar to that of *hGBPs* and *mGbps* (Degrandi et al., 2007; Kim et al., 2011; Olszewski et al., 2006).

3.4. Upregulation of tGBPs expression by virus infections

The GBPs have been shown to be important mediators of host defense *in vivo* against bacteria and parasites, and are involved in antiviral innate immunity (Pilla-Moffett et al., 2016). We examined the mRNA alterations of *tGBPs* in response to different virus infections in TSPRCs. Either the RNA virus (NDV or EMCV) or DNA virus (HSV-1) infection stimulated *tGBPs* mRNA expression (Fig. 5). NDV infection significantly and persistently upregulated all five *tGBPs* as early as 9 h post infection (hpi) (Fig. 5A). EMCV infection significantly induced *tGBPs* expression at 12 hpi, and *tGBP1* and *tGBP5* had an earlier upregulation at 9 hpi (Fig. 5B). HSV-1 infection continuously enhanced the mRNA expression of *tGBPs* at 6 hpi (Fig. 5C). Among these three viruses, NDV infection had the most pronounced effect (Fig. 5). These results suggested that *tGBPs* were upregulated by viral infections and might play active roles in antiviral immunity.

3.5. Cellular location of tGBPs

The cellular location was important for GBP proteins to exert their host defense function against pathogen infection (Biering et al., 2017; Choi et al., 2016; Park et al., 2016; Wandel et al., 2017; Yamamoto et al., 2012). We investigated cellular location of tGBPs in TSPRCs with or without viral infections. The tGBPs were widely distributed in the cytoplasm of TSPRCs, and this localization pattern was not altered by NDV or HSV-1 infection (Fig. 6). Overexpression of tGBP7 showed seemingly granular structures irrespective of viral infections, which might be the aggregation of overexpressed tGBP7 protein (Fig. 6) (Britzen-Laurent et al., 2010). We could not examine the cellular localization of endogenous tGBPs due to the lack of workable antibodies for detecting individual tGBPs.

3.6. Overexpression of tGBP1 repressed VSV replication in TSPRCs

The GBPs of human and mouse have been shown to be involved in

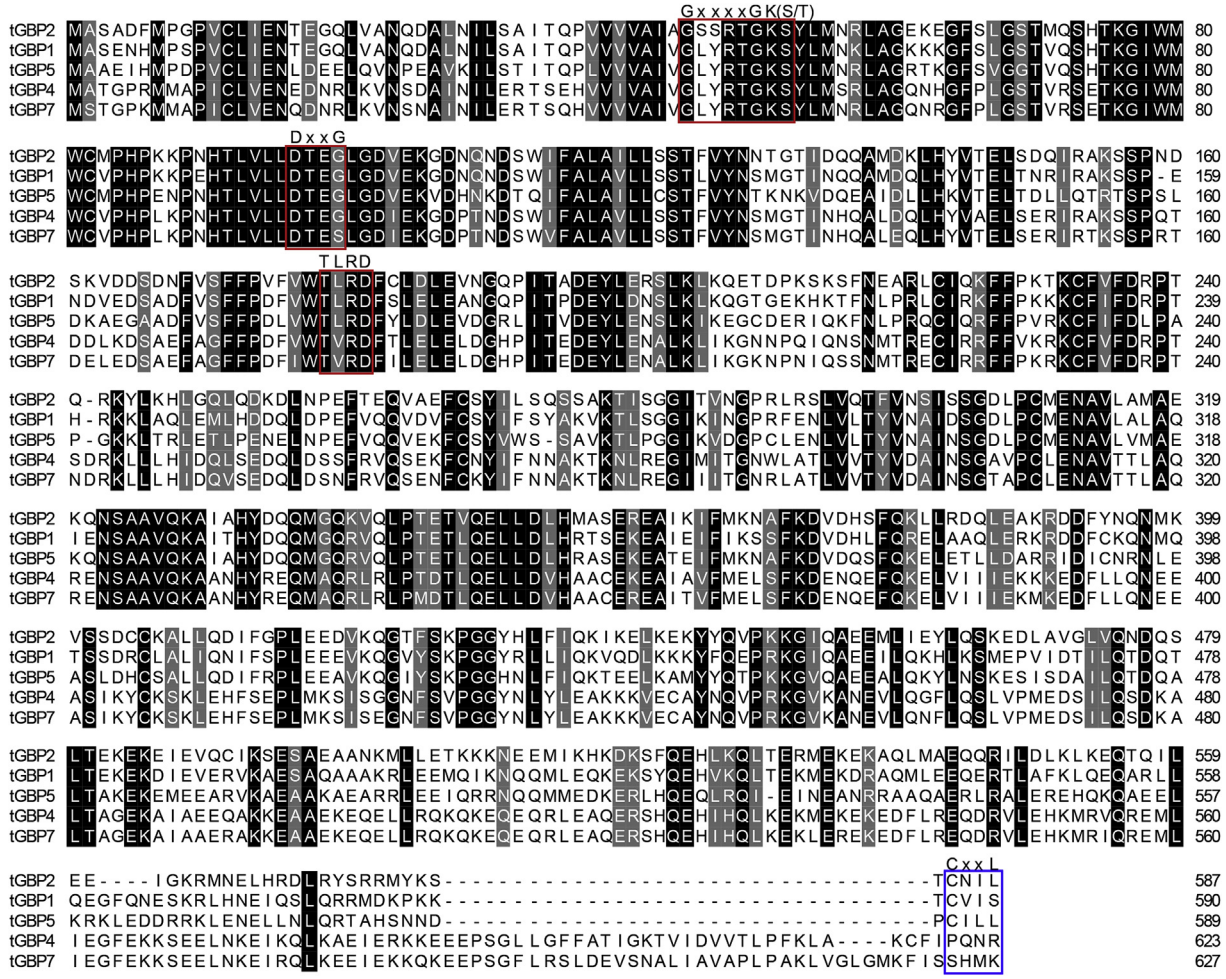

Fig. 2. Multiple protein sequence alignment of five tGBPs. Black boxes indicated identical residues, and gray boxes indicated similar residues. The three conserved motifs within the GTP-binding site and the carboxy-terminal CaaX motif were marked in red box and blue box, respectively. (For interpretation of the references to colour in this figure legend, the reader is referred to the Web version of this article.)

the response against viral infection (Pilla-Moffett et al., 2016). We examined the antiviral function of tGBPs upon VSV and HSV-1 infections. TSPRCs were transiently transfected with respective tGBP expression vector. All 5 tGBPs could be successfully overexpressed in TSPRCs (Fig. 7A). As had been reported before (Xu et al., 2015, 2016), overexpression of tMAVS or tMITA (as a positive control) inhibited VSV and HSV-1 infection, respectively (Fig. 7B–D). Ectopic expression of tGBP1 significantly inhibited the replication of VSV and had a mild effect on HSV-1 replication in TSPRCs (Fig. 7B–D). However, the other tGBPs had no apparent inhibitory effect on VSV and HSV-1 replications (Fig. 7B–D).

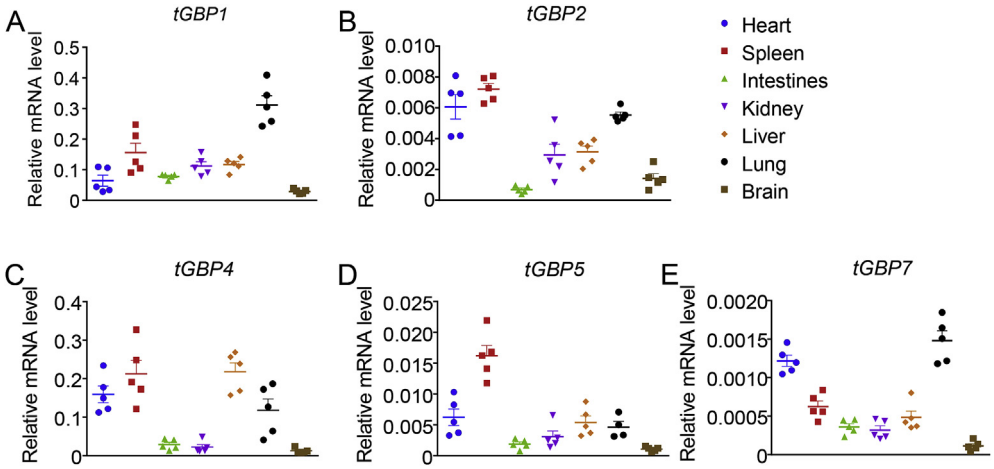

Fig. 3. The mRNA levels of *tGBPs* in seven tissues of the Chinese tree shrews. The mRNA levels of (A) *tGBP1*, (B) *tGBP2*, (C) *tGBP4*, (D) *tGBP5* and (E) *tGBP7* in each tissue from five healthy adult tree shrews were measured by quantitative real-time PCR, with normalization to *β-actin*.

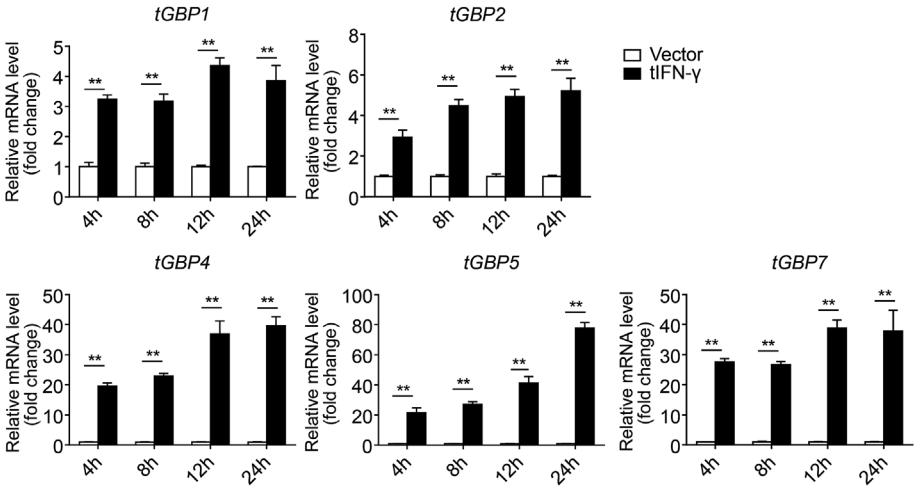

Fig. 4. Upregulation of *tGBP* mRNA expression in tree shrew primary renal cells (TSPRCs) with and without tIFN-γ treatment. The TSPRCs were stimulated by culture supernatants of HEK293T cells transfected with pCMV-3tag-8 (empty vector) or pCMV-tIFNγ-3tag-8 for the indicated times. The relative mRNA levels of *tGBPs* were determined by quantitative real-time PCR, with normalization to *β-actin*. The fold values (relative to the controls at each time point) were presented as mean ± SEM. The experiments were repeated three times, with consistent results.

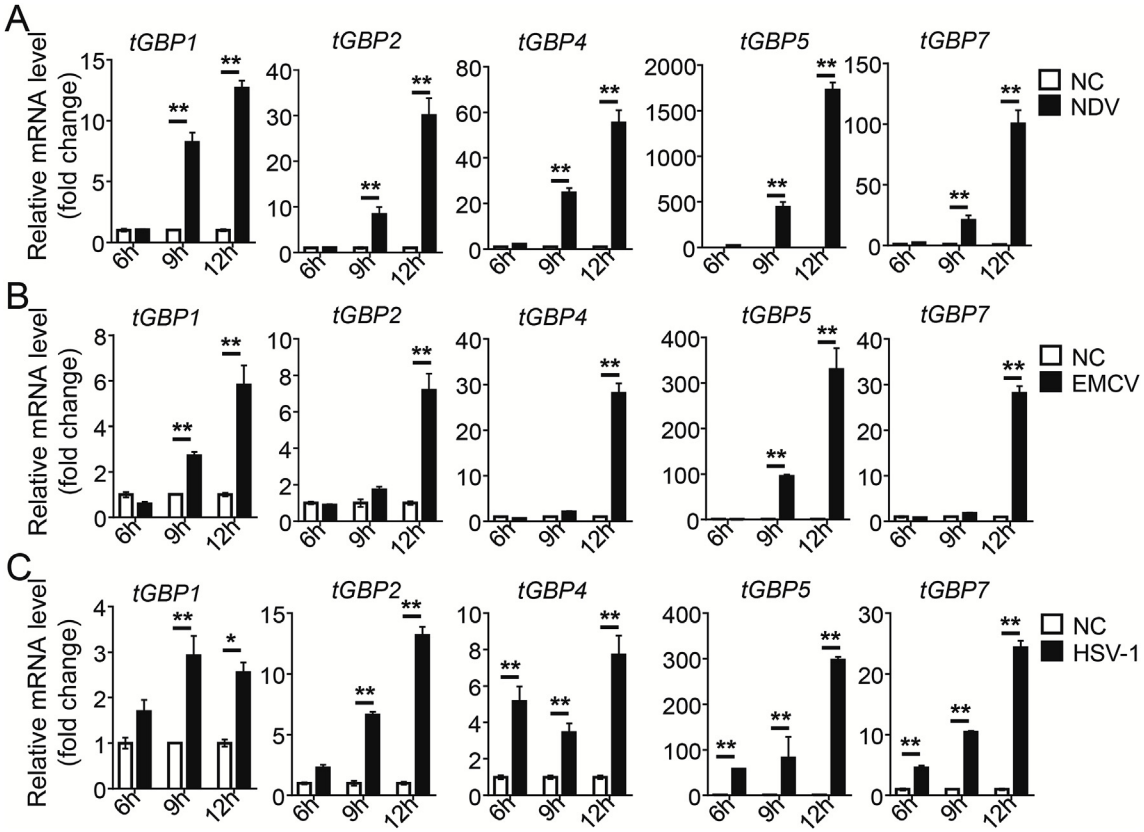

Fig. 5. Upregulation of mRNA levels of *tGBPs* in tree shrew primary renal cells (TSPRCs) in response to virus infections. The TSPRCs were infected by (A) NDV (MOI = 1), (B) EMCV (MOI = 1) or (C) HSV-1 (MOI = 1) for the indicated time points. The mRNA level of each *tGBP* was determined by quantitative real-time PCR, with normalization to *β-actin*. Data shown were fold changes of each *tGBP* relative to the respective control. The experiments were repeated three times with similar results.

3.7. Knockout of tGBP1 promoted VSV replication in a tree shrew renal cell line

We further confirmed the antiviral activity of tGBP1 by knocking out this gene in the TSR6 cell line, which was immortalized from TSPRCs in our recent study (Gu et al., 2019). Using the CRISPR/Cas9 technique, we successfully disrupted the *tGBP1* coding frame by introducing mutation c.74_75insA (Fig. 8A). As expected, the VSV replication was significantly increased in the TSR6 cells with tGBP1 knockout relative to wild-type cells (Fig. 8B and C). Collectively, these results based on the overexpression and knockout of tGBP1 supported its antiviral activity.

4. Discussion

In recent years, the Chinese tree shrew has received much attention in the field for its usage as a small and viable experimental animal (Li et al., 2018; Yao, 2017). The closer affinity of the tree shrew to primates as compared to that of rodents to primates had opened a new avenue for replacing primates by tree shrew in biomedical researches in certain aspects (Xiao et al., 2017; Yao, 2017), especially considering the recent breakthrough for gene editing (Ma et al., 2018) and transgenic

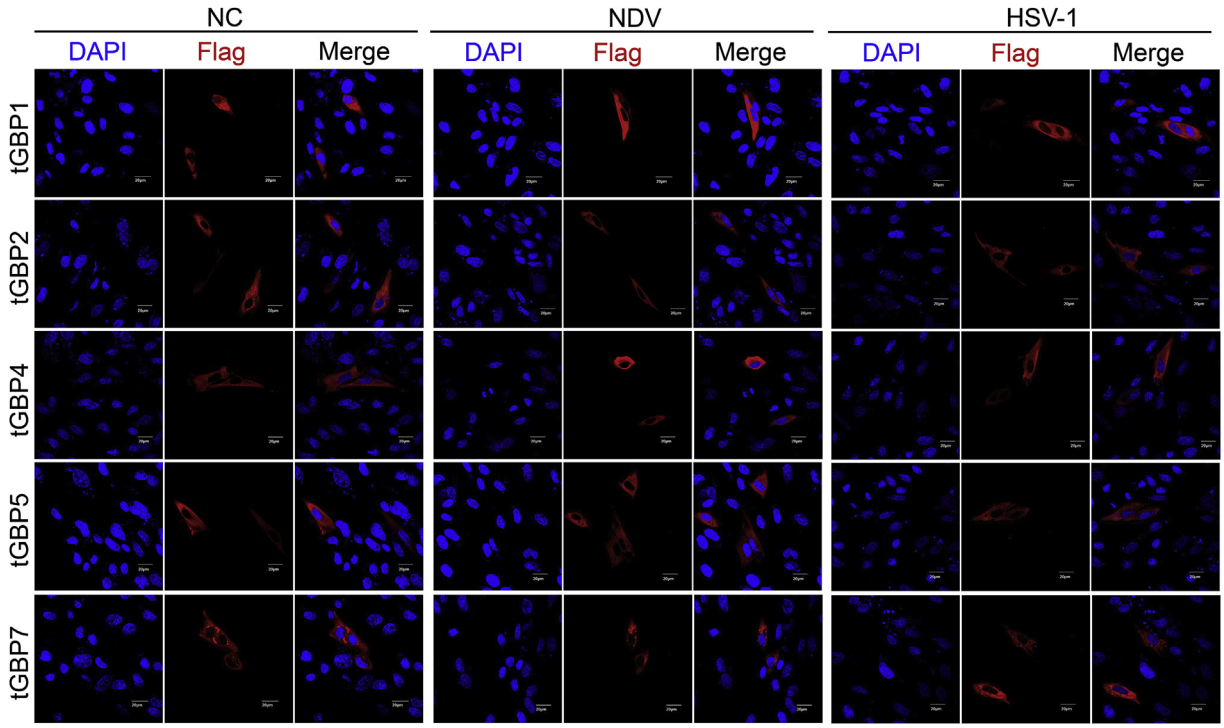

Fig. 6. Cellular localization of tGBPs in tree shrew renal cells (TSPRCs) with or without viral infections. Cells were transiently transfected with the indicated Flag-tagged tGBP expression vector for 24 h, then were infected with NDV (MOI = 1) or HSV-1 (MOI = 1) for 12 h. After fixation and immunostaining, cellular localization of the respective tGBP was examined using confocal microscope. Data shown were representative of three independent experiments.

manipulation of the Chinese tree shrews (Li et al., 2017; Xu et al., 2017). We and others have described the unique and common features of the tree shrew immune genes in the recent years (Jiang et al., 2018; Luo et al., 2018; Mu et al., 2014; Xu et al., 2016; Yao et al., 2019; Yu et al., 2014, 2016). In this study, we characterized the GBPs in the Chinese tree shrew, and we added another case showing the conservation and divergence of GBPs in tree shrew.

GBPs play important roles in host defense against bacterial, parasitic and viral pathogens (Meunier and Broz, 2016; Pilla-Moffett et al., 2016). However, the *GBP* family were only well characterized in human and mouse (Degrandi et al., 2007; Olszewski et al., 2006). Homologs of *GBPs* were not detected in any invertebrate species, indicating that *GBPs* were most likely arose in the ancestor of chordates and functioned only in vertebrate species (Olszewski et al., 2006; Pilla-Moffett et al., 2016). Five *GBPs* were successfully identified in the Chinese tree shrew. These tGBPs shared the common features with hGBPs and mGbps. The most conserved GTP binding motif TLRD/TVRD and GxxxxGK(S/T) (Degrandi et al., 2007; Olszewski et al., 2006; Pilla-Moffett et al., 2016) were presented in all tGBPs. In accordance with hGBPs and mGbps, tGBP1, tGBP2 and tGBP5 had a CaaX motif in the C-terminal parts (Olszewski et al., 2006). Further analysis demonstrated that the *GBPs* in tree shrew had a closer relationship with *hGBPs* than with *mGbps*. First, the chromosomal location and gene organization of *tGBPs* were more similar to *hGBPs* compared to *mGbps* (Kim et al., 2011; Olszewski et al., 2006; Pilla-Moffett et al., 2016). Second, the phylogenetic clustering pattern of *tGBPs* with *hGBPs* also supported this conclusion. These observations were in line with the opinion that the Chinese tree shrew had a close relationship with primates (Fan et al., 2013; Xu et al., 2013a).

Hitherto, the tissue expression patterns of *GBPs* had not been fully evaluated in other species except for human and mouse (Degrandi et al., 2007; Kim et al., 2011; Olszewski et al., 2006). The expression profiles of *GBPs* in human and mouse had been compared by using the data form UniGene database (Olszewski et al., 2006), which showed that *hGBP1* and *mGbp2* in the spleen and *hGBP4* and *mGbp3* in the bone marrow had a similar expression pattern, respectively (Olszewski et al., 2006). We examined the tissue expression profiles of *tGBPs* in seven tissues from healthy adult tree shrews and provided the first-hand data for the tissue expression pattern of *GBPs*. The *tGBPs* were ubiquitously expression in all seven tissues examined in this study, but there was a tissue-specific pattern for different members. The overall tissue expression pattern of *tGBPs* resembled that of human (Olszewski et al., 2006).

GBPs are ISGs that were induced by many cytokines and proinflammatory cytokines, and were mainly induced by IFN-γ (Degrandi et al., 2007; Tripal et al., 2007). Similarly to *hGBPs* and *mGbps*, *tGBPs* were strongly induced by tIFN-γ. In addition, mRNA levels of *tGBPs* could be stimulated by virus infections, suggesting that *tGBPs* are involved in the antiviral immune response. It has been reported that GBPs were recruited to the pathogen-containing vacuoles (PCVs) to destruct the integrity of PCVs, thus to expose the pathogens to host or to eliminate it (Choi et al., 2014; Kravets et al., 2016). Previous studies showed that hGBP1 and hGBP5 were consistently located in cytoplasm in the resting state or upon different virus infections (Feng et al., 2017; Itsui et al., 2009; Zou et al., 2017). Porcine GBP1 also showed a similar cellular location in response to classical swine fever virus infection (Li et al., 2016c). Consistent with these observations, we found that tGBPs were located in the cytoplasm and viral infections had no apparent effect on the cellular localization of tGBPs.

Human GBP1 showed antiviral activity against various virus infections, such as VSV, EMCV, HCV, KSHV and HBV (Anderson et al., 1999; Itsui et al., 2009; Lu et al., 2008; Zou et al., 2017). While the tGBP1 had an inhibitory effect on VSV and HSV-1 replications, the other tGBPs had no obvious effect on the replications of VSV and HSV-1. We speculated that tGBP1 and hGBP1 may share the same antiviral mechanism, as *tGBP1* and *hGBP1* had a closer affinity in the phylogenetic tree, and both presented similar antiviral spectrum (Anderson et al., 1999; Carter et al., 2005; Itsui et al., 2009). The antiviral activity of hGBP1 against the positive-strand RNA virus and DNA virus infections had been well depicted (Itsui et al., 2009; Zou et al., 2017). As VSV is a negative-strand RNA virus, further functional assays should be performed to

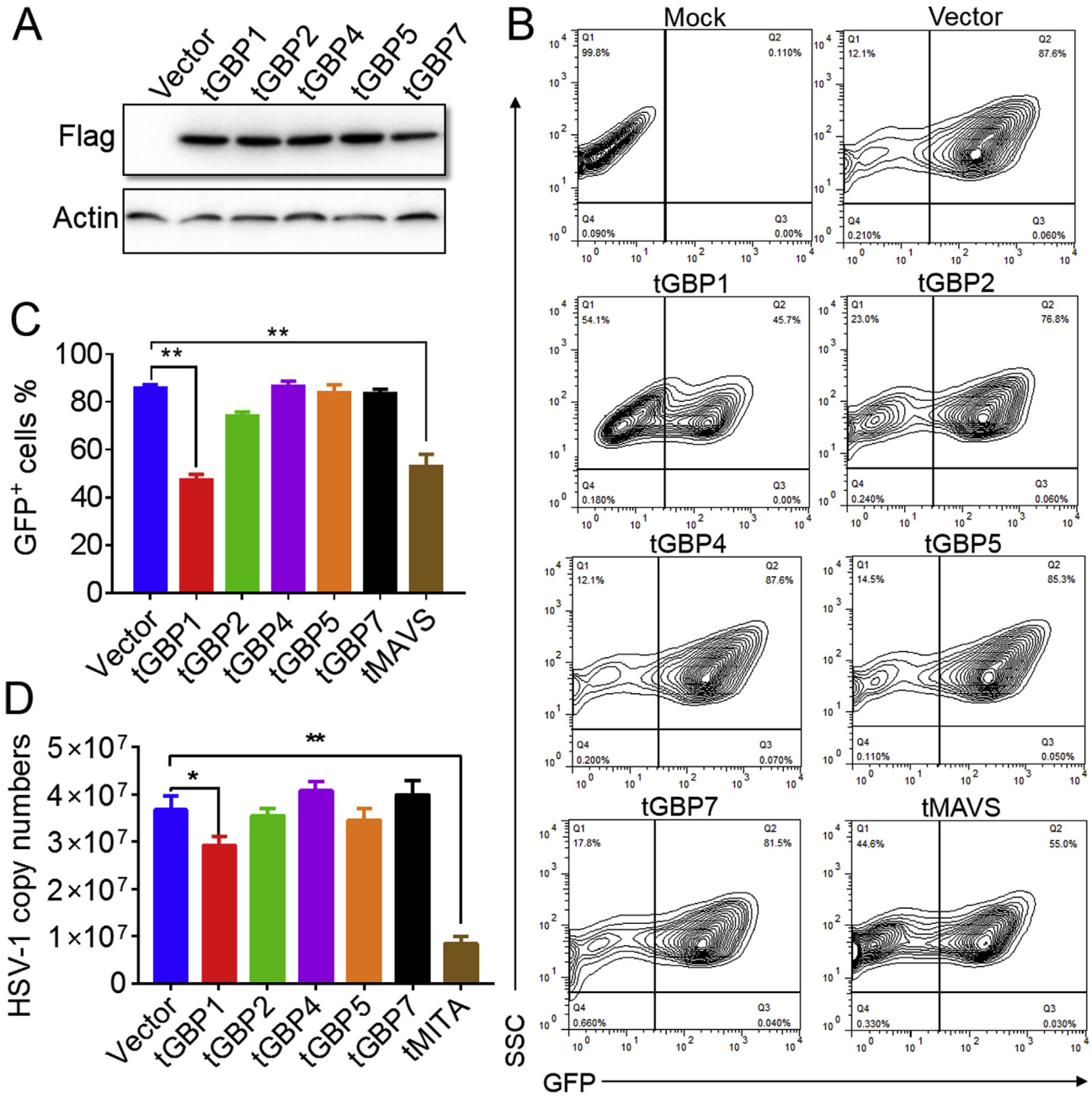

Fig. 7. Overexpression of tGBP1 inhibited replication of VSV and HSV-1 in tree shrew renal cells (TSPRCs). (A) Western blot analysis of the overexpressed tGBPs in TSPRCs. (B) Flow cytometry analysis and (C) quantification of VSV replication in TSPRCs overexpressing the indicated vector. Cells (1×10^5) were transfected with the indicated vector (1 μg) for 12 h before being infected with VSV-GFP (MOI = 0.01) for 12 h. Percentage of 10,000 cells expressing GFP (GFP^+ cells) was counted by flow cytometry. Overexpression of tMAVS was used as a positive control. (D) Quantification of HSV-1 replication in TSPRCs overexpressing the indicated vectors. TSPRCs (1×10^5) were transfected with the indicated vectors for 24 h, followed by infection with HSV-1 (MOI = 1) for 1 h. Cells were washed three times with PBS and switched to growth medium for 24 h. The copy number of HSV-1 DNA in the culture supernatant was analyzed by quantitative real-time PCR using the specific primers for HSV-1 genome as reported in previous study (Zhang et al., 2014). Overexpression of tMITA was used as a positive control. The data were representative of three independent experiments.

understand the antiviral function of tGBP1 against VSV infection. This pursuit will benefit for the understanding of the broad antiviral spectrum of GBP1.

In short, we identified five *tGBPs* and confirmed the conservation of GBP structure and function in the Chinese tree shrew. The updated information about the GBPs in the Chinese tree shrew will provide more information for the GBP family and for us to learn the innate immune restriction factors in this species.

Conflicts of interest

The authors declare no conflict of interest.

Acknowledgments

This study was supported by the National Natural Science Foundation of China (U1402224 to Y-GY, 31700155 to LX), Yunnan Province (2016FB018 to LX) and CAS “Light of West China” Program (to LX).

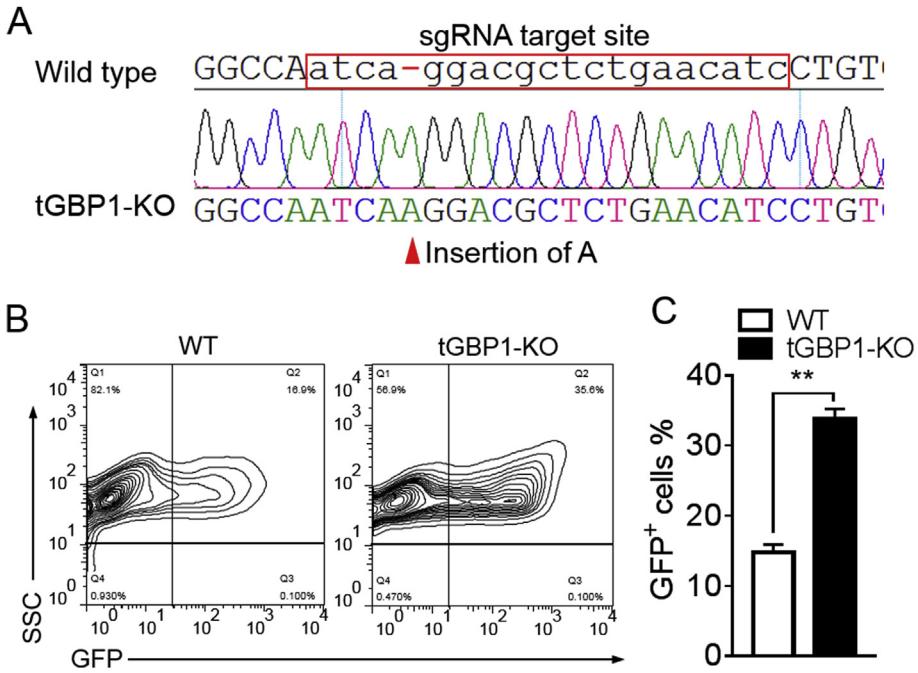

Fig. 8. Knockout of *tGBP1* promotes VSV replication in tree shrew renal cell line TSR6. (A) Sequencing chromatographs showing the mutation in the *tGBP1* gene in TSR6 cells with gene editing (tGBP1-KO) and the unedited TSR6 cells (WT, wild type). (B) Flow cytometry analysis and (C) quantification of VSV replication in TSR6 cells with (tGBP1-KO) or without (WT) deficiency of tGBP1. Cells were infected with VSV-GFP (MOI = 0.01) for 12 h. Percentage of 10,000 cells expressing GFP (GFP^+ cells) was counted by flow cytometry. The data were representative of three independent experiments.

Appendix A. Supplementary data

Supplementary data to this article can be found online at https://doi.org/10.1016/j.dci.2019.02.014.

References

Akira, S., Uematsu, S., Takeuchi, O., 2006. Pathogen recognition and innate immunity. Cell 124, 783–801.

Anderson, S.L., Carton, J.M., Lou, J., Xing, L., Rubin, B.Y., 1999. Interferon-induced guanylate binding protein-1 (GBP-1) mediates an antiviral effect against vesicular stomatitis virus and encephalomyocarditis virus. Virology 256, 8–14.

Biering, S.B., Choi, J., Halstrom, R.A., Brown, H.M., Beatty, W.L., Lee, S., McCune, B.T., Dominici, E., Williams, L.E., Orchard, R.C., Wilen, C.B., Yamamoto, M., Coers, J., Taylor, G.A., Hwang, S., 2017. Viral replication complexes are targeted by LC3-guided interferon-inducible GTPases. Cell Host Microbe 22, 74–85 e77.

Borden, E.C., Sen, G.C., Uze, G., Silverman, R.H., Ransohoff, R.M., Foster, G.R., Stark, G.R., 2007. Interferons at age 50: past, current and future impact on biomedicine. Nat. Rev. Drug Discov. 6, 975–990.

Britzen-Laurent, N., Bauer, M., Berton, V., Fischer, N., Syguda, A., Reipschläger, S., Naschberger, E., Herrmann, C., Stürzl, M., 2010. Intracellular trafficking of guanylate-binding proteins is regulated by heterodimerization in a hierarchical manner. PLoS One 5 e14246.

Carter, C.C., Gorbacheva, V.Y., Vestal, D.J., 2005. Inhibition of VSV and EMCV replication by the interferon-induced GTPase, mGBP-2: differential requirement for wild-type GTP binding domain. Arch. Virol. 150, 1213–1220.

Choi, J., Biering, S.B., Hwang, S., 2016. Quo vadis? Interferon-inducible GTPases go to their target membranes via the LC3-conjugation system of autophagy. Small GTPases 8, 199–207.

Choi, J., Park, S., Biering, S.B., Selleck, E., Liu, C.Y., Zhang, X., Fujita, N., Saitoh, T., Akira, S., Yoshimori, T., Sibley, L.D., Hwang, S., Virgin, H.W., 2014. The parasitophorous vacuole membrane of *Toxoplasma gondii* is targeted for disruption by ubiquitin-like conjugation systems of autophagy. Immunity 40, 924–935.

Degrandi, D., Konermann, C., Beuter-Gunia, C., Kresse, A., Wurthner, J., Kurig, S., Beer, S., Pfeffer, K., 2007. Extensive characterization of IFN-induced GTPases mGBP1 to mGBP10 involved in host defense. J. Immunol. 179, 7729–7740.

Edgar, R.C., 2004. MUSCLE: multiple sequence alignment with high accuracy and high throughput. Nucleic Acids Res. 32, 1792–1797.

Fan, Y., Huang, Z.Y., Cao, C.C., Chen, C.S., Chen, Y.X., Fan, D.D., He, J., Hou, H.L., Hu, L., Hu, X.T., Jiang, X.T., Lai, R., Lang, Y.S., Liang, B., Liao, S.G., Mu, D., Ma, Y.Y., Niu, Y.Y., Sun, X.Q., Xia, J.Q., Xiao, J., Xiong, Z.Q., Xu, L., Yang, L., Zhang, Y., Zhao, W., Zhao, X.D., Zheng, Y.T., Zhou, J.M., Zhu, Y.B., Zhang, G.J., Wang, J., Yao, Y.G., 2013. Genome of the Chinese tree shrew. Nat. Commun. 4, 1426.

Fan, Y., Luo, R., Su, L.Y., Xiang, Q., Yu, D., Xu, L., Chen, J.Q., Bi, R., Wu, D.D., Zheng, P., Yao, Y.G., 2018. Does the genetic feature of the Chinese tree shrew (*Tupaia belangeri chinensis*) support its potential as a viable model for alzheimer's disease research? J. Alzheimers Dis. 61, 1015–1028.

Fan, Y., Yu, D., Yao, Y.G., 2014. Tree shrew database (TreeshrewDB): a genomic knowledge base for the Chinese tree shrew. Sci. Rep. 4, 7145.

Feng, J., Cao, Z., Wang, L., Wan, Y., Peng, N., Wang, Q., Chen, X., Zhou, Y., Zhu, Y., 2017. Inducible GBP5 mediates the antiviral response via interferon-related pathways during influenza A virus infection. J. Innate Immun. 419–435.

Goubau, D., Deddouche, S., Reis, E.S.C., 2013. Cytosolic sensing of viruses. Immunity 38, 855–869.

Gu, T., Yu, D., Li, Y., Xu, L., Yao, Y.-L., Yao, Y.-G., 2019. Establishment and characterization of an immortalized renal cell line of the Chinese tree shrew (*Tupaia belangeri chinesis*). Appl. Microbiol. Biotechnol. https://doi.org/10.1007/s00253-00019-09615-00253.

Guo, W.N., Zhu, B., Ai, L., Yang, D.L., Wang, B.J., 2018. Animal models for the study of hepatitis B virus infection. Zool. Res. 39, 25–31.

Hotter, D., Sauter, D., Kirchhoff, F., 2017. Guanylate binding protein 5: impairing virion infectivity by targeting retroviral envelope glycoproteins. Small GTPases 8, 31–37.

Hu, Y., Wang, J., Yang, B., Zheng, N., Qin, M., Ji, Y., Lin, G., Tian, L., Wu, X., Wu, L., Sun, B., 2011. Guanylate binding protein 4 negatively regulates virus-induced type I IFN and antiviral response by targeting IFN regulatory factor 7. J. Immunol. 187, 6456–6462.

Itsui, Y., Sakamoto, N., Kakinuma, S., Nakagawa, M., Sekine-Osajima, Y., Tasaka-Fujita, M., Nishimura-Sakurai, Y., Suda, G., Karakama, Y., Mishima, K., Yamamoto, M., Watanabe, T., Ueyama, M., Funaoka, Y., Azuma, S., Watanabe, M., 2009. Antiviral effects of the interferon-induced protein guanylate binding protein 1 and its interaction with the hepatitis C virus NS5B protein. Hepatology 50, 1727–1737.

Jiang, Z., Gao, B., Hu, M., Ding, L., Lan, Z., Yu, M., Yu, H., Cui, Q., Lin, J., Li, M., 2018. Conserved structure and function of chemokine CXCL8 between Chinese tree shrews and humans. Gene 677, 149–162.

Kim, B.H., Shenoy, A.R., Kumar, P., Bradfield, C.J., MacMicking, J.D., 2012. IFN-inducible GTPases in host cell defense. Cell Host Microbe 12, 432–444.

Kim, B.H., Shenoy, A.R., Kumar, P., Das, R., Tiwari, S., MacMicking, J.D., 2011. A family of IFN-gamma-inducible 65-kD GTPases protects against bacterial infection. Science 332, 717–721.

Krapp, C., Hotter, D., Gawanbacht, A., McLaren, P.J., Kluge, S.F., Sturzel, C.M., Mack, K., Reith, E., Engelhart, S., Ciuffi, A., Hornung, V., Sauter, D., Telenti, A., Kirchhoff, F., 2016. Guanylate binding protein (GBP) 5 is an interferon-inducible inhibitor of HIV-1 infectivity. Cell Host Microbe 19, 504–514.

Kravets, E., Degrandi, D., Ma, Q., Peulen, T.O., Klumpers, V., Felekyan, S., Kuhnemuth, R., Weidtkamp-Peters, S., Seidel, C.A., Pfeffer, K., 2016. Guanylate binding proteins directly attack *Toxoplasma gondii* via supramolecular complexes. Elife 5.

Li, C.H., Yan, L.Z., Ban, W.Z., Tu, Q., Wu, Y., Wang, L., Bi, R., Ji, S., Ma, Y.H., Nie, W.H., Lv, L.B., Yao, Y.G., Zhao, X.D., Zheng, P., 2017. Long-term propagation of tree shrew spermatogonial stem cells in culture and successful generation of transgenic offspring. Cell Res. 27, 241–252.

Li, J.P., Liao, Y., Zhang, Y., Wang, J.J., Wang, L.C., Feng, K., Li, Q.H., Liu, L.D., 2014. Experimental infection of tree shrews (*Tupaia belangeri*) with Coxsackie virus A16. Zool. Res. 35, 485–491.

Li, L., Li, Z., Li, X., Wang, E., Lang, F., Xia, Y., Fraser, N.W., Gao, F., Zhou, J., 2016a. Reactivation of HSV-1 following explant of tree shrew brain. J. Neurovirol. 22, 293–306.

Li, L., Li, Z., Wang, E., Yang, R., Xiao, Y., Han, H., Lang, F., Li, X., Xia, Y., Gao, F., Li, Q., Fraser, N.W., Zhou, J., 2016b. Herpes simplex virus 1 infection of tree shrews differs from that of mice in the severity of acute infection and viral transcription in the peripheral nervous system. J. Virol. 90, 790–804.

Li, L.F., Yu, J., Li, Y., Wang, J., Li, S., Zhang, L., Xia, S.L., Yang, Q., Wang, X., Yu, S., Luo, Y., Sun, Y., Zhu, Y., Munir, M., Qiu, H.J., 2016c. Guanylate-binding protein 1, an

interferon-induced GTPase, exerts an antiviral activity against classical swine fever virus depending on its GTPase activity. J. Virol. 90, 4412–4426.
Li, R., Zanin, M., Xia, X., Yang, Z., 2018. The tree shrew as a model for infectious diseases research. J. Thorac. Dis. 10, S2272–s2279.
Lu, Y.P., Wang, B.J., Dong, J.H., Liu, Z., Guan, S.H., Lu, M.J., Yang, D.L., 2008. Antiviral effect of interferon-induced guanylate binding protein-1 against coxsackie virus and hepatitis B virus B3 *in vitro*. Virol. Sin. 22, 193.
Luo, M.T., Fan, Y., Mu, D., Yao, Y.G., Zheng, Y.T., 2018. Molecular cloning and characterization of APOBEC3 family in tree shrew. Gene 646, 143–152.
Ma, X., Wong, A.S., Tam, H.Y., Tsui, S.Y., Chung, D.L., Feng, B., 2018. *In vivo* genome editing thrives with diversified CRISPR technologies. Zool. Res. 39, 58–71.
MacMicking, J.D., 2004. IFN-inducible GTPases and immunity to intracellular pathogens. Trends Immunol. 25, 601–609.
McNab, F., Mayer-Barber, K., Sher, A., Wack, A., O'Garra, A., 2015. Type I interferons in infectious disease. Nat. Rev. Immunol. 15, 87–103.
Meunier, E., Broz, P., 2016. Interferon-inducible GTPases in cell autonomous and innate immunity. Cell Microbiol. 18, 168–180.
Mu, D., Yang, H., Zhu, J.W., Liu, F.L., Tian, R.R., Zheng, H.Y., Han, J.B., Shi, P., Zheng, Y.T., 2014. Independent birth of a novel TRIMCyp in *Tupaia belangeri* with a divergent function from its paralog TRIM5. Mol. Biol. Evol. 31, 2985–2997.
Nordmann, A., Wixler, L., Boergeling, Y., Wixler, V., Ludwig, S., 2012. A new splice variant of the human guanylate-binding protein 3 mediates anti-influenza activity through inhibition of viral transcription and replication. FASEB J. 26, 1290–1300.
Oliveros, J.C., Franch, M., Tabas-Madrid, D., San-Leon, D., Montoliu, L., Cubas, P., Pazos, F., 2016. Breaking-Cas-interactive design of guide RNAs for CRISPR-Cas experiments for ENSEMBL genomes. Nucleic Acids Res. 44, W267–W271.
Olszewski, M.A., Gray, J., Vestal, D.J., 2006. *In silico* genomic analysis of the human and murine guanylate-binding protein (GBP) gene clusters. J. Interferon Cytokine Res. 26, 328–352.
Park, S., Choi, J., Biering, S.B., Dominici, E., Williams, L.E., Hwang, S., 2016. Targeting by AutophaGy proteins (TAG): targeting of IFNG-inducible GTPases to membranes by the LC3 conjugation system of autophagy. Autophagy 12, 1153–1167.
Pilla-Moffett, D., Barber, M.F., Taylor, G.A., Coers, J., 2016. Interferon-inducible GTPases in host resistance, inflammation and disease. J. Mol. Biol. 428, 3495–3513.
Ran, F.A., Hsu, P.D., Wright, J., Agarwala, V., Scott, D.A., Zhang, F., 2013. Genome engineering using the CRISPR-Cas9 system. Nat. Protoc. 8, 2281–2308.
Schneider, W.M., Chevillotte, M.D., Rice, C.M., 2014. Interferon-stimulated genes: a complex web of host defenses. Annu. Rev. Immunol. 32, 513–545.
Tamura, K., Stecher, G., Peterson, D., Filipski, A., Kumar, S., 2013. MEGA6: molecular evolutionary genetics analysis version 6.0. Mol. Biol. Evol. 30, 2725–2729.
Tripal, P., Bauer, M., Naschberger, E., Mortinger, T., Hohenadl, C., Cornali, E., Thurau, M., Sturzl, M., 2007. Unique features of different members of the human guanylate-binding protein family. J. Interferon Cytokine Res. 27, 44–52.
Tsukiyama-Kohara, K., Kohara, M., 2014. *Tupaia belangeri* as an experimental animal model for viral infection. Exp. Anim. 63, 367–374.
Walter, E., Keist, R., Niederost, B., Pult, I., Blum, H.E., 1996. Hepatitis B virus infection of *tupaia* hepatocytes *in vitro* and *in vivo*. Hepatology 24, 1–5.
Wandel, M.P., Pathe, C., Werner, E.I., Ellison, C.J., Boyle, K.B., von der Malsburg, A., Rohde, J., Randow, F., 2017. GBPs inhibit motility of *shigella flexneri* but are targeted for degradation by the bacterial ubiquitin ligase IpaH9.8. Cell Host Microbe 22, 507–518.
Wang, Q., Schwarzenberger, P., Yang, F., Zhang, J., Su, J., Yang, C., Cao, J., Ou, C., Liang, L., Shi, J., Yang, F., Wang, D., Wang, J., Wang, X., Ruan, P., Li, Y., 2012. Experimental chronic hepatitis B infection of neonatal tree shrews (*Tupaia belangeri chinensis*): a model to study molecular causes for susceptibility and disease progression to chronic hepatitis in humans. Virol. J. 9, 170.
Wei, S., Hua, H.R., Chen, Q.Q., Zhang, Y., Chen, F., Li, S.Q., Li, F., Li, J.L., 2017. Dynamic changes in DNA demethylation in the tree shrew (*Tupaia belangeri chinensis*) brain during postnatal development and aging. Zool. Res. 38, 96–102.
Xiao, J., Liu, R., Chen, C.S., 2017. Tree shrew (*Tupaia belangeri*) as a novel laboratory disease animal model. Zool. Res. 38, 127–137.
Xie, Z.C., Riezu-Boj, J.I., Lasarte, J.J., Guillen, J., Su, J.H., Civeira, M.P., Prieto, J., 1998. Transmission of hepatitis C virus infection to tree shrews. Virology 244, 513–520.
Xu, D., Zhu, Y., Xu, Z., 2017. Efficient genetic manipulation in the developing brain of tree shrew using in utero electroporation and virus infection. J. Genet. Genomics. 44, 507–509.
Xu, L., Fan, Y., Jiang, X.L., Yao, Y.G., 2013a. Molecular evidence on the phylogenetic position of tree shrews. Zool. Res. 34, 70–76.
Xu, L., Yu, D., Fan, Y., Peng, L., Wu, Y., Yao, Y.G., 2016. Loss of RIG-I leads to a functional replacement with MDA5 in the Chinese tree shrew. Proc. Natl. Acad. Sci. U. S. A 113, 10950–10955.
Xu, L., Yu, D., Peng, L., Fan, Y., Chen, J., Zheng, Y.T., Wang, C., Yao, Y.G., 2015. Characterization of a MAVS ortholog from the Chinese tree shrew (*Tupaia belangeri chinensis*). Dev. Comp. Immunol. 52, 58–68.
Xu, L., Zhang, Y., Liang, B., Lu, L.B., Chen, C.S., Chen, Y.B., Zhou, J.M., Yao, Y.G., 2013b. Tree shrews under the spot light: emerging model of human diseases. Zool. Res. 34, 59–69.
Yamamoto, M., Okuyama, M., Ma, J.S., Kimura, T., Kamiyama, N., Saiga, H., Ohshima, J., Sasai, M., Kayama, H., Okamoto, T., Huang, David C.S., Soldati-Favre, D., Horie, K., Takeda, J., Takeda, K., 2012. A cluster of interferon-γ-inducible p65 GTPases plays a critical role in host defense against *toxoplasma gondii*. Immunity 37, 302–313.
Yan, R.Q., Su, J.J., Huang, D.R., Gan, Y.C., Yang, C., Huang, G.H., 1996. Human hepatitis B virus and hepatocellular carcinoma. I. experimental infection of tree shrews with hepatitis B virus. J. Canc. Res. Clin. Oncol. 122, 283–288.
Yang, Z.F., Zhao, J., Zhu, Y.T., Wang, Y.T., Liu, R., Zhao, S.S., Li, R.F., Yang, C.G., Li, J.Q., Zhong, N.S., 2013. The tree shrew provides a useful alternative model for the study of influenza H1N1 virus. Virol. J. 10, 111.
Yao, Y.G., 2017. Creating animal models, why not use the Chinese tree shrew (*Tupaia belangeri chinensis*)? Zool. Res. 38, 118–126.
Yao, Y.L., Yu, D., Xu, L., Fan, Y., Wu, Y., Gu, T., Chen, J., Lv, L.B., Yao, Y.G., 2019. Molecular characterization of the 2',5'-oligoadenylate synthetase family in the Chinese tree shrew (*Tupaia belangeri chinensis*). Cytokine. https://doi.org/10.1016/j.cyto.2018.1011.1009.
Yu, D., Wu, Y., Xu, L., Fan, Y., Peng, L., Xu, M., Yao, Y.G., 2016. Identification and characterization of toll-like receptors (TLRs) in the Chinese tree shrew (*Tupaia belangeri chinensis*). Dev. Comp. Immunol. 60, 127–138.
Yu, D., Xu, L., Liu, X.H., Fan, Y., Lu, L.B., Yao, Y.G., 2014. Diverse interleukin-7 mRNA transcripts in Chinese tree shrew (*Tupaia belangeri chinensis*). PLoS One 9 e99859.
Zhang, G.Q., Ge, X.N., Guo, X., Yang, H.C., 2007. Genomic analysis of two porcine encephalomyocarditis virus strains isolated in China. Arch. Virol. 152, 1209–1213.
Zhang, L., Mo, J., Swanson, K.V., Wen, H., Petrucelli, A., Gregory, S.M., Zhang, Z., Schneider, M., Jiang, Y., Fitzgerald, K.A., Ouyang, S., Liu, Z.J., Damania, B., Shu, H.B., Duncan, J.A., Ting, J.P., 2014. NLRC3, a member of the NLR family of proteins, is a negative regulator of innate immune signaling induced by the DNA sensor STING. Immunity 40, 329–341.
Zheng, Y.T., Yao, Y.G., Xu, L., 2014. Basic Biology and Disease Models of Tree Shrews. Yunnan Science and Technology Press, Kunming.
Zou, Z., Meng, Z., Ma, C., Liang, D., Sun, R., Lan, K., 2017. Guanylate-binding protein 1 inhibits nuclear delivery of kaposi's sarcoma-associated herpesvirus virions by disrupting formation of actin filament. J. Virol. 91 e00632–17.

Table S1. Primers used in this study

Gene	Usage	Primer sequence (5' - 3')
tGBP1	5' RACE	TTTATGTTTTTCACCAGTACCTTGC
	5' RACE nest	GCTGTTATACACTAAGGTGCTGCTC
	3' RACE	CTGTGATTGATACAATTCTACAGAC
	3' RACE nest	AAAGAGCATATCTGTCATCCTTACT
	RT-qPCR F	TTTGATCGACCCACTCACCG
	RT-qPCR R	AGTGGGTAATGGCCTTCTGC
	Vector construction F	ATGC*ggatcc*ATGGCCTCAGAGAACCACAT
	Vector construction R	ATGC*ctcgag*ACTTATGACACATGTCTTCTTTGGC
tGBP2	5' RACE	AGGTGTGGTTTGGCTTCTTGGGATG
	5' RACE nest	CGCAATAGCCACCACCACGACA
	3' RACE	GGAGATAGGGAAACGGATGAATGAA
	3' RACE nest	ATGGGAGAGATCATGCAGGTTCTGT
	RT-qPCR F	TCAGCAGACTTCATGCCAGG
	RT-qPCR R	AATAGCCACCACCACGACAG
	Vector construction F	ATGC*gatatc*ATGGCCTCAGCAGACTTCAT
	Vector construction R	ATGC*gtcgac*GAGTATGTTACATGTTGATTTGTACA
tGBP4	5' RACE	CCTTTTCTATGTCGCCCAGGCTCT
	5' RACE nest	TTCTGTCCAGCCAGGCGGTTCAT
	3' RACE	TCATTTTGAAGTATATGCGTATTAG
	3' RACE nest	CTTTTAAATCAGTGAGAAGCGAGCA
	RT-qPCR F	TACCTAGGCCACTGAGCACT
	RT-qPCR R	ACCACATCCAGATGCCCTTG
	Vector construction F	ATGC*gatatc*ATGATGGCCCCCATATGTCTAG
	Vector construction R	ATGC*ctcgag*TTTCATATGTGAACTGATAAATTTC
tGBP5	5' RACE	AAATCTGGGTGTCCTTGTTGTGGTC
	5' RACE nest	GCATACACCACATCCAGATTCCCT
	3' RACE	CCAGGCTCTCACAGCGAAGGAAA
	3' RACE nest	CCATCAGGAACAACTCAGACAAATAGA
	RT-qPCR F	CCCTACTAGATGCAAGGCGG
	RT-qPCR R	ACTCCTTTCTTGGGCGTCTG
	Vector construction F	ATGC*ggatcc*CTCGGAAAGGTCTCCACCCCCAAT
	Vector construction R	ATGC*ctcgag*AATACTTCGAAGTAAGATACATGGGTCA
tGBP7	5' RACE	TGACCACATGCTCAGATGTCCTTTC
	5' RACE nest	CTCCTGGGAAACTGACTGTTCTTAG
	3' RACE	ACAGCACCTAACAGTCAAAACACAA
	3' RACE nest	ATTTTGAAAAGTGGAACCAGATTAG
	RT-qPCR F	AGGTTGCTGTGCTAGATCCC
	RT-qPCR R	TCTTGGGCAGACAGGCAATG
	Vector construction F	ATGC*ggatcc*ATGGCAACTGGACCCAGGAT
	Vector construction R	ATGC*ctcgag*TCGGTTTTGTGGAATGAAGCAT
tIFNγ	Vector construction F	ATGC*ggatcc*ATGAAGTATACAAGTTATACACTGG
	Vector construction R	ATGC*ctcgag*TCTGGAAGCTCTCCGACCT

The nucleotides marked in italic refer to the recognition site of restricted enzymes. RT-qPCR, quantitative real-time PCR.

Table S2. The characteristics of tree shrew GBPs

Gene name	5′ UTR (bp)	3′ UTR (bp)	CDS (bp)	Full-length (bp)	Mw (kD)	GenBank accession number
tGBP1	816	196	1733	2155	67.6	MK214685
tGBP2	127	1162	1764	3052	66.9	MK214686
tGBP4	323	728	1872	2922	71.3	MK214687
tGBP5	218	134	1770	2120	67.3	MK214688
tGBP7	126	719	1884	2728	71.4	MK214689

Mw, molecular weight.